Accepted manuscript doi:
10.1680/jgele.18.00114

Submitted: 26 June 2018

Published online in 'accepted manuscript' format: 12 November 2018

Manuscript title: Hydro-mechanical behaviour of high-density bentonite pellet upon partial hydration

Authors: B. Darde*†, A. M. Tang*, J.-M. Pereira*, J.-N. Roux*, P. Dangla*, J. Talandier† and M. N. Vu†

Affiliations: *Université Paris-Est, Laboratoire Navier, UMR 8205 (Ecole des Ponts ParisTech – Ifsttar – CNRS), Marne-la-Vallée, France and †French National Radioactive Waste Management Agency (Andra), Châtenay-Malabry, France

Corresponding author: Anh Minh Tang, Ecole des Ponts ParisTech, Laboratoire Navier/Géotechnique (CERMES), 6-8 avenue Blaise Pascal, 77455 MARNE-LA-VALLEE, France. Tel.: +33 1 64 15 35 63.

E-mail: anh-minh.tang@enpc.fr

Accepted manuscript doi:
10.1680/jgele.18.00114

Abstract

The hydro-mechanical behaviour of a high-density bentonite pellet, potential candidate for engineered barriers in high-level radioactive waste disposal, is investigated through laboratory tests. Water content and volumetric strain are first determined at various suctions (ranging from 9 MPa to 89 MPa) during partial hydration from its initial state. Afterward, compression tests allow the Young modulus and strength to be determined at various suctions. The experimental results are then interpreted by using an existing model describing the hydro-mechanical behaviour of an aggregate in compacted expansive clay. The analyses show that a single set of parameters is sufficient to predict the suction dependency of volumetric strain, Young modulus and compressive strengths. These findings would be helpful for further numerical investigations on the hydro-mechanical behaviour of granular bentonite-based engineered barriers by using both finite element and discrete element methods.

Keywords: Partial saturation; Expansive soils; Laboratory tests

Accepted manuscript doi:
10.1680/jgele.18.00114

Introduction

Bentonite-based materials are considered as candidate materials for engineered barriers in radioactive waste disposal due to their low permeability, good radionuclides retention capacity, and ability to swell upon hydration, which is an important property to fill the technological voids. While many studies on the hydro-mechanical behaviour of bentonite-based engineered barriers have focused on compacted blocks of bentonite, bentonite pellets/powder mixtures have also been considered as an interesting alternative (Volckaert et al., 1996; van Geet et al., 2005; Imbert and Villar, 2006; Hoffman et al., 2007; Alonso et al., 2011; Gens et al., 2011; Molinero-Guerra et al., 2017).

After Kröhn (2005), vapour diffusion plays a significant – if not dominant – role in the resaturation process of bentonite-based engineered barriers. In order to study the hydro-mechanical behaviour of bentonite pellets mixtures upon hydration by vapour transfer, accounting for the granular nature of the material (Molinera-Guerra et al., 2018*a*,*b*), numerical simulations based on the discrete element method (DEM) (Cundall and Strack, 1979; Roux and Chevoir, 2005; Agnolin and Roux, 2007; Than et al., 2017) could be an interesting way of assessing the influence of pellets swelling on the mixtures behaviour. In DEM simulations, each particle is modelled individually. A model describing the hydro-mechanical behaviour of a single pellet is therefore required. As this approach is valid for granular materials, the model has to focus on hydration state at which a pellet has not lost its initial structure.

For this purpose, the present study focuses on the hydro-mechanical behaviour of a single pellet upon partial hydration. The vapour equilibrium technique is used to hydrate the pellet. At equilibrium, the pellet volume and water content are determined, which allows determining the relationship between volumetric strain and suction. Afterward, a compression test is performed on the pellet to determine its stiffness and strength. Finally, the results are interpreted through the conceptual framework proposed by Alonso et al. (1999).

2. Material

The material characterised in this study are sub-spherical MX80 bentonite pellets. MX80 is a Na-bentonite from Wyoming, with high smectite contents, which main physical properties are summarised in Table 1. Pellets are obtained through compaction of bentonite powder. They are composed of a cylinder-shaped part and two spherical ends (Figure 1). Their initial properties are shown in Table 2.

3. Experimental methods

Suction-controlled hydration is performed through the vapour equilibrium technique (Tang and Cui, 2005; Delage et al., 2006). Pellets are placed within a desiccator containing a saturated salt solution. When equilibrium is reached (verified by pellet mass), the pellets dimensions are measured using a camera (one picture is taken from the side, Figure 1a, and pellet's height and diameter are measured with an accuracy of 0.01 mm). Axial strain ε_a and radial strain ε_r are determined by comparison of height and diameter with their initial values. Volumetric strain ε_V is calculated as follows:

$$\varepsilon_V = (1+\varepsilon_a)(1+\varepsilon_r)^2 - 1 \qquad (1)$$

Compression tests are carried out by using a load frame (Figure 2). The displacement rate is imposed at 0.1 mm/min. Displacements are recorded by a displacement transducer and the

Accepted manuscript doi:
10.1680/jgele.18.00114

contact force between the pellet and the frame is recorded by a force transducer (with an accuracy of 0.1 N).

Compression tests are performed in both axial and radial directions (Figure 3). In axial compression tests (Figure 3a), contact between the load frame and the pellet is sub-punctual. Assuming isotropic linear elastic behaviour, the Hertz law is adapted to obtain Young modulus (Johnson, 1985):

$$N = \frac{1}{3}\frac{E}{1-\nu^2}\left(2R_c\right)^{1/2}\delta_n^{3/2} \quad (2)$$

Where N is the axial load; E and ν are Young modulus and Poisson's ratio, respectively; δ_n is the normal displacement.

In radial compression test (Figure 3b), the contact is assumed to be linear. Johnson (1985)'s elasticity law, relating normal displacement to normal force for a contact between an infinite plate and a cylinder, is applied to determine E.

$$\delta_n = 2\frac{N}{h}\frac{1-\nu^2}{\pi E}\left[2\ln\left(2\sqrt{\frac{\frac{\pi D}{2}\frac{E}{1-\nu^2}}{\frac{N}{h}}}\right)-1\right] \quad (3)$$

Figure 4 presents the results corresponding to s = 89 MPa. Several tests are performed and one curve is chosen to show the method for determination of E. For axial compression tests (Figure 4a), N increases with increasing displacement until failure. At failure, N decreases abruptly. The Hertz law (equation 2) is then used to fit experimental data from the start to the failure to determine E. In the present work, ν = 0.3 for the sake of simplicity. For radial compression tests (Figure 4b), N increases with increasing displacement in two distinct phases: first, a slow increase; second, a more significant and sub-linear increase. The first phase is interpreted as the consequence of an imperfect contact between the frame and the pellet at the beginning of the test. As displacement increases, the contact becomes linear and the force-displacement relationship is significantly modified. Considering this hypothesis, equation (3) is used to fit experimental data only from the start of the second phase to the failure.

In the present work, beside the initial suction, eight suctions (ranging from 9 MPa to 82 MPa) are considered. For each one, several pellets are analysed to assess the repeatability of the experimental data.

4. Experimental results

Figure 5 presents w versus elapsed time during the suction equilibrium phase. From its initial value (12.2%), w increases quickly during the first days and equilibrium is reached after 10 days, except for the lowest suction (9 MPa) where 30 days were necessary. The values obtained at equilibrium (Figure 5) are then plotted versus imposed suction in Figure 6*a*. Along the hydration path (decrease of suction from 89 MPa to 9 MPa) w increases from 12.2 % to 24.3 %. Results obtained on the same materials (MX80) in other studies are also plotted. Within the investigated suction range, w - s relationships are similar and do not depend on the initial dry density or hydration conditions. Figure 6*b* presents the degree of saturation (S_r) versus suction which shows that S_r does not change significantly during this hydration phase. Figure 7 presents the strains versus suction during this hydration phase. ε_a is generally higher than ε_r. The mean values of ε_v, obtained from the mean values of ε_a and ε_r, are plotted. As expected, ε_v keeps increasing upon hydration.

Accepted manuscript doi:
10.1680/jgele.18.00114

The mechanical properties (*E* and strength) are plotted versus suction in Figure 8. Moduli obtained for both axial and radial compression tests are similar (Figure 8*a*) and a single mean value is retained for both compression directions. These results confirm that the assumptions used to interpret the compression tests (isotropic linear elastic behaviour, equations 2 & 3) are appropriate. Upon hydration, the pellet modulus and strength decrease significantly. Finally, the relationship between compressive strengths and modulus is presented in Figure 9. A linear relationship is suggested for both axial and radial directions.

5. Model

In the present work, the pellet initial dry density is high and its behaviour is assumed to be similar to that of an aggregate (*i.e.* the microstructural level) in compacted expansive clay following the model proposed by Alonso et al. (1999).

Microstructural volumetric strain is written:

$$\mathrm{d}\varepsilon_{\mathrm{vm}} = \frac{\mathrm{d}\hat{p}}{K_m} = \frac{\mathrm{d}s}{K_m} \tag{4}$$

$$K_m(s) = \frac{1}{\beta_m}\ \exp(\alpha_m\ s) \tag{5}$$

Where K_m is the microstructural bulk modulus, $\hat{p}$ is the effective mean stress (equal to s in the present study), α_m and β_m are material parameters.

From compression tests results, α_m = 0.024 MPa^{-1} and β_m = 0.016 MPa^{-1} are obtained through basic exponential regression (Figure 8a).

Integrating (5) from initial suction s_0 to a given suction s leads to:

$$\varepsilon_{vm} = \frac{\beta_m}{\alpha_m}\left[\exp\left(-\alpha_m\ s_0\right) - \exp\left(-\alpha_m\ s\right)\right] \tag{6}$$

Where α_m and β_m values, determined from compression tests results, are found to satisfactorily model the volumetric strain upon hydration (Figure 7).

From Figure 9, it seems convenient to propose a linear relationship between pellet strengths and modulus. The following relationships are proposed:

$$R_A = C_A E \tag{7}$$

$$R_R = C_R E \tag{8}$$

where C_A and C_R are material parameters relating the strength to the modulus for axial and radial compression tests, respectively. C_A = 1.206×10^{-7} m^{-2} and C_R = 1.816×10^{-7} m^{-2} following the fitting (Figure 9).

From (5), (7) and (8), the evolution of pellet strength upon hydration can be written:

$$R_A = 3(1-2\nu)C_A \frac{1}{\beta_m}\exp(\alpha_m s) \tag{9}$$

$$R_R = 3(1-2\nu)C_R \frac{1}{\beta_m}\exp(\alpha_m s) \tag{10}$$

Model predictions are presented in dash lines in Figure 9, along experimental results for comparison.

6. Discussion

The experimental results show that partial hydration induces an increase in water content and pellet volume and a decrease in Young modulus and strength. These trends agree with existing results on bentonite-based materials (Wiebe et al., 1998; Blatz et al., 2002; Lloret et al., 2003; Tang and Cui, 2009; Carrier et al., 2016). However, the volumetric strain obtained in the present work (50% for hydration from 89 MPa to 9 MPa) is higher than that observed on a single MX80 bentonite aggregate (25%, after Tang and Cui 2009). In addition, the Young modulus measured in the present work is generally one order of magnitude smaller than that measured by Carrier et al. (2016) on MX80 bentonite clay film over the same suction range. It means that the mechanical behaviour of the material is strongly dependent on the dimensions of the specimen.

In addition, it is interesting to note that the results obtained by compression tests (Figure 8a) can be used to predict the results obtained by hydration (Figure 7). The role of total stress is thus similar to that of suction as suggested by Alonso et al. (1999) for microstructural level. The present work contributes to a more comprehensive approach to model the behaviour of a single pellet. These results would be helpful for further numerical investigations on the hydro-mechanical behaviour of granular bentonite using the finite element method with double-porosity models (i.e. Alonso et al., 2011) where a single pellet corresponds to the micro-structural level. Actually, Molinero Guerra et al. (2017) performed mercury intrusion porosimetry on a similar bentonite pellet and found that the volume of macro-pores is negligible at high suction. Besides, for numerical investigations using discrete element modelling, these results can be directly used to describe the behaviour of a single pellet under hydro-mechanical loading.

However, it is worthy to mention that the behaviour of the pellet observed in the present work doesn't correspond to all the assumptions proposed for an aggregate in the model of Alonso et al. (1999): (*i*) the pellet is not fully-saturated; (*ii*) its behaviour is not reversible; (*iii*) the volumetric behaviour of the pellet is not isotropic. In spite of these disagreements, the model would correctly predict the hydro-mechanical behaviour of a pellet during this partial hydration path (up to 9 MPa of suction). At suction lower than this value, the model would no longer be valid as the pellet would disaggregate (as suggested by Saiyouri et al. 2004 for bentonite particles, Koliji et al., 2010 and Cardoso et al., 2013 for clay aggregates less reactive than bentonite).

In addition to the volumetric behaviour, the strengths of the pellet under compression can be also predicted by using the same values of α_m and β_m. These results can be explained by the linear correlation between the strengths and the modulus. Actually, correlations between these two properties were observed on various compacted clayey soils (Lee et al., 2005; Zeh and Witt, 2007).

7. Conclusions

The behaviour of a single high-density bentonite pellet under hydration from 82 to 9 MPa of suction and the variation of its mechanical properties during this path are investigated in this study by laboratory tests. The results show an increase of pellet's volume and water content upon suction decrease. At the same time, its mechanical properties (Young modulus and strengths) decrease during hydration. When analysing the experimental result with an existing model for compacted expansive soil and assuming that the pellet behaviour is similar to that of an aggregate, a single set of parameters (α_m and β_m) can be used to predict the suction dependency of volumetric strain, Young modulus and strengths.

The results from this work would be helpful for further numerical investigations (finite element and discrete element methods) on the hydro-mechanical behaviour of granular bentonite-based engineered barrier for geological radioactive waste disposal during the first years following the installation.

List of notations

ρ_s	particle density
ρ_d	dry density
e	void ratio
w	water content
D	pellet's diameter
H	pellet's total height
h	pellet's cylinder-shaped part height
Rc	pellet's curvature radius
s_0	initial suction
ε_a	axial strain
ε_r	radial strain
ε_V	volumetric strain
N	axial load
E	Young modulus
v	Poisson ratio
δ_n	normal displacement
S_r	degree of saturation
R_R	normal force at failure during radial compression
R_A	normal force at failure during axial compression
K_m	microstructural bulk modulus
$\hat{p}$	effective mean stress
α_m	material parameter
β_m	material parameter
C_A	material parameter relating axial strength to modulus
C_R	material parameter relating radial strength to modulus

References

Agnolin, I., & Roux, J. N. (2007). Internal states of model isotropic granular packings. I. Assembling process, geometry, and contact networks. Physical Review E - Statistical, Nonlinear, and Soft Matter Physics, 76(6), 1–27. https://doi.org/10.1103/PhysRevE.76.061302

Alonso, E. E., Vaunat, J., & Gens, A. (1999). Modelling the mechanical behaviour of expansive clays. Engineering Geology, 54(1–2), 173–183. https://doi.org/10.1016/S0013-7952(99)00079-4

Alonso, E. E., Romero, E., & Hoffmann, C. (2011). Hydromechanical behaviour of compacted granular expansive mixtures: experimental and constitutive study. Géotechnique, 61(4), 329–344. https://doi.org/10.1680/geot.2011.61.4.329

Blatz, J. A., Graham, J., & Chandler, N. A. (2002). Influence of suction on the strength and stiffness of compacted sand-bentonite. Canadian Geotechnical Journal, 39(5), 1005–1015. https://doi.org/10.1139/t02-056

Cardoso, R., Alonso, E.E, and Maranha das Neves, E. (2013) A constitutive model for compacted expansive and bonded marls. Géotechnique, 63(13), 1116 – 1130. https://doi.org/10.1680/geot.12.P.101

Cundall, P., & Strack, O. (1979). A discrete numerical model for granular assemblies. Géotechnique, 29(1), 47–65.

Delage, P., Marcial, D., Ruiz, X., & Cui, Y. J. (2006). Ageing effects in a compacted bentonite: a microstructure approach. Géotechnique, 56(5), 291–304. https://doi.org/10.1680/geot.2006.56.5.291

Gens, A., Valleján, B., Sánchez, M., Imbert, C., Villar, M. V., & Van Geet, M. (2011). Hydromechanical behaviour of a heterogeneous compacted soil: experimental

observations and modelling. Géotechnique, 61(5), 367–386. https://doi.org/10.1680/geot.SIP11.P.015

Hoffmann, C., Alonso, E. E., & Romero, E. (2007). Hydro-mechanical behaviour of bentonite pellet mixtures. Physics and Chemistry of the Earth, 32(8–14), 832–849. https://doi.org/10.1016/j.pce.2006.04.037

Imbert, C., & Villar, M. V. (2006). Hydro-mechanical response of a bentonite pellets/powder mixture upon infiltration. Applied Clay Science, 32(3–4), 197–209. https://doi.org/10.1016/j.clay.2006.01.005

Johnson, K. L. (1985). Contact Mechanics. Cambridge, UK: Cambridge University Press. https://doi.org/10.1115/1.3261297

Koliji, A., Laloui, L. and Vulliet, L. (2010), Constitutive modeling of unsaturated aggregated soils. Int. J. Numer. Anal. Meth., 34, 1846 – 1876. https://doi.org/10.1002/nag.888

Kröhn, K. P. (2005). New evidence for the dominance of vapour diffusion during the re-saturation of compacted bentonite. Engineering Geology, 82(2), 127–132. https://doi.org/10.1016/j.enggeo.2005.09.015

Lee, F. H., Lee, Y., Chew, S.-H., & Yong, K. Y. (2005). Strength and modulus of marine clay-cement mixes. Journal of Geotechnical and Geoenvironmental Engineering, 131(2), 178–186. https://doi.org/10.1061/(ASCE)1090-0241(2005)131:2(178)

Lloret, A., Villar, M. V, Sanchez, M., Gens, A., Pintado, X., & Alonso, E. (2003). Mechanical behaviour of heavily compacted bentonite under high suction changes. Geotechnique, 53(1), 27–40. https://doi.org/10.1680/geot.53.1.27.37258

Molinero Guerra, A., Mokni, N., Delage, P., Cui, Y. J., Tang, A. M., Aimedieu, P., Bornert, M. (2017). In-depth characterisation of a mixture composed of powder/pellets MX80

bentonite. Applied Clay Science, 135, 538–546. https://doi.org/10.1016/j.clay.2016.10.030

Molinero-Guerra, A., Aimedieu, P., Bornert, M, Cui, Y.J., Tang, A.M., Sun, Z., Mokni, N., Delage, P., Bernier, F. (2018a). Analysis of the structural changes of a pellet/powder bentonite mixture upon wetting by X-ray computed microtomography. Applied Clay Science. (doi: 10.1016/j.clay.2018.07.043)

Molinero-Guerra, A., Cui, Y.J., Mokni, N., Delage, P., Bornert, M., Aimedieu, P., Tang, A.M., & Bernier, F. (2018b). Investigation of the hydro-mechanical behaviour of a pellet/powder MX80 bentonite mixture using an infiltration column. Engineering Geology, 243, 18 – 25.

Roux, J.-N., & Chevoir, F. (2005). Généralités sur la simulation numérique discrète des matériaux granulaires, 254, 109–138.

Saiyouri, N., Tessier, D., & Hicher, P. Y. (2004). Experimental study of swelling in unsaturated compacted clays. Clay Minerals, 39(4), 469–479. https://doi.org/10.1180/0009855043940148

Tang, A.-M., & Cui, Y.-J. (2005). Controlling suction by the vapour equilibrium technique at different temperatures and its application in determining the water retention properties of MX80 clay. Canadian Geotechnical Journal, 42(1), 287–296. https://doi.org/10.1139/t04-082

Tang, A.M., Cui, Y.J. (2009). Modelling the thermo-mechanical behaviour of compacted expansive clays. Géotechnique, 59 (3), 185-195. (doi: 10.1680/geot.2009.59.3.185)

Than, V.D., Khamseh, S., Tang, A.M., Pereira, J.M., Chevoir, F., & Roux, J.N. (2017). Basic Mechanical Properties of Wet Granular Materials: A DEM Study. J. Eng. Mech.,143(1), C4016001. (doi:10.1061/(ASCE)EM.1943-7889.0001043).

Van Geet, M., Volckaert, G., & Roels, S. (2005). The use of microfocus X-ray computed tomography in characterising the hydration of a clay pellet/powder mixture. Applied Clay Science, 29(2), 73–87. https://doi.org/10.1016/j.clay.2004.12.007

Volckaert, G., Bernier, F., Alonso, E. E., Gens, A., Samper, J., Villar, M. V., Martin-Martin, P. L., Cuevas, J., Campos, R., Thomas, H., Imbert, C. & Zingarelli, V. (1996). Thermal-hydraulic-mechanical and geochemical behaviour of the clay barrier in radioactive waste repositories (model development and validation), EUR 16744 EN. Luxembourg: Publications of the European Communities.

Wiebe, B., Graham, J., Tang, G. X., & Dixon, D. (1998). Influence of pressure, saturation, and temperature on the behaviour of unsaturated sand-bentonite. Canadian Geotechnical Journal, 35, 194–205. https://doi.org/10.1139/t97-093

Zeh, R. M., & Witt, K. J. (2007). The tensile strength of compacted clays as affected by suction and soil structure. Experimental Unsaturated Soil Mechanics, 112, 219–226. https://doi.org/10.1007/3-540-69873-6_21

Table captions

Table 1. Physical properties of MX80 bentonite
Table 2. Initial properties of the pellets

Table 1 Physical properties of MX80 bentonite

Property	**Value**
Particle density, ρs (Mg/m3)	2.77
Smectite content (%)	80
Liquid limit (%)	560
Plastic limit (%)	53
CEC (meq/g)	98/100

Accepted manuscript doi:
10.1680/jgele.18.00114

Table 2 Initial properties of the pellets

Property	**Value**
Dry density, ρd (Mg/m3)	1.90
Void ratio, e (-)	0.46
Water content, w (%)	12.2
Diameter, D (mm)	7.0
Height, H (mm)	7.0
Height of the cylinder-shaped part, h (mm)	5.0
Curvature radius, Rc (mm)	6.5
Suction, s0 (MPa)	89

Figure captions

Figure 1. Schematic views of a single pellet. Radial view (a) and axial view (b).

Figure 2. Load frame used to perform compression test. (a) Picture; (b) description

Figure 3. Schematic view of the compression tests: (a) axial compression; (b) radial compression.

Figure 4. Typical results of compression tests: (a) axial compression; (b) radial compression.

Figure 5. Water content versus elapsed time during the suction equilibrium phase.

Figure 6. (a) Water content versus suction; (b) Degree of saturation versus suction.

Figure 7. Axial, radial and volumetric strains versus suction.

Figure 8: (a) Modulus versus suction for axial and radial compression tests; (b) Strength versus suction for axial and radial compression tests.

Figure 9: Strength versus modulus for both axial and radial compression tests.

Accepted manuscript doi:
10.1680/jgele.18.00114

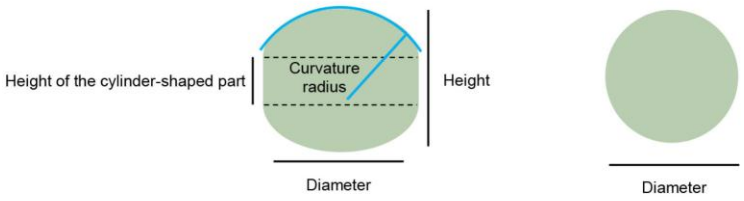

a) b)

Figure_1.tif

Accepted manuscript doi:
10.1680/jgele.18.00114

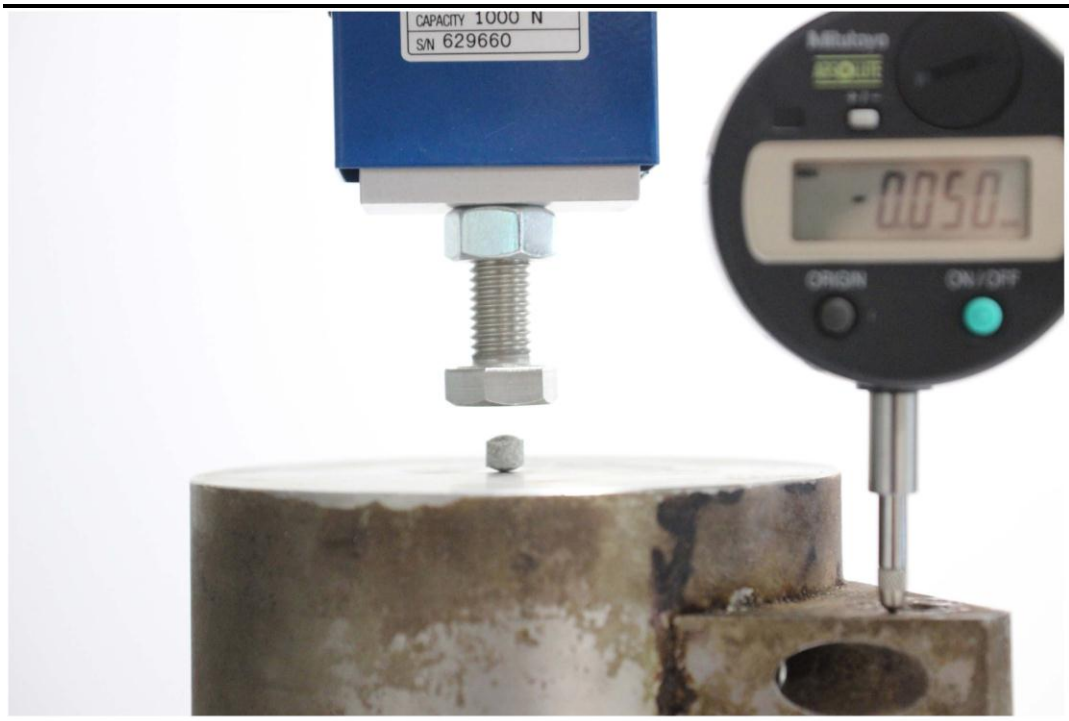

figure_2_a.JPG

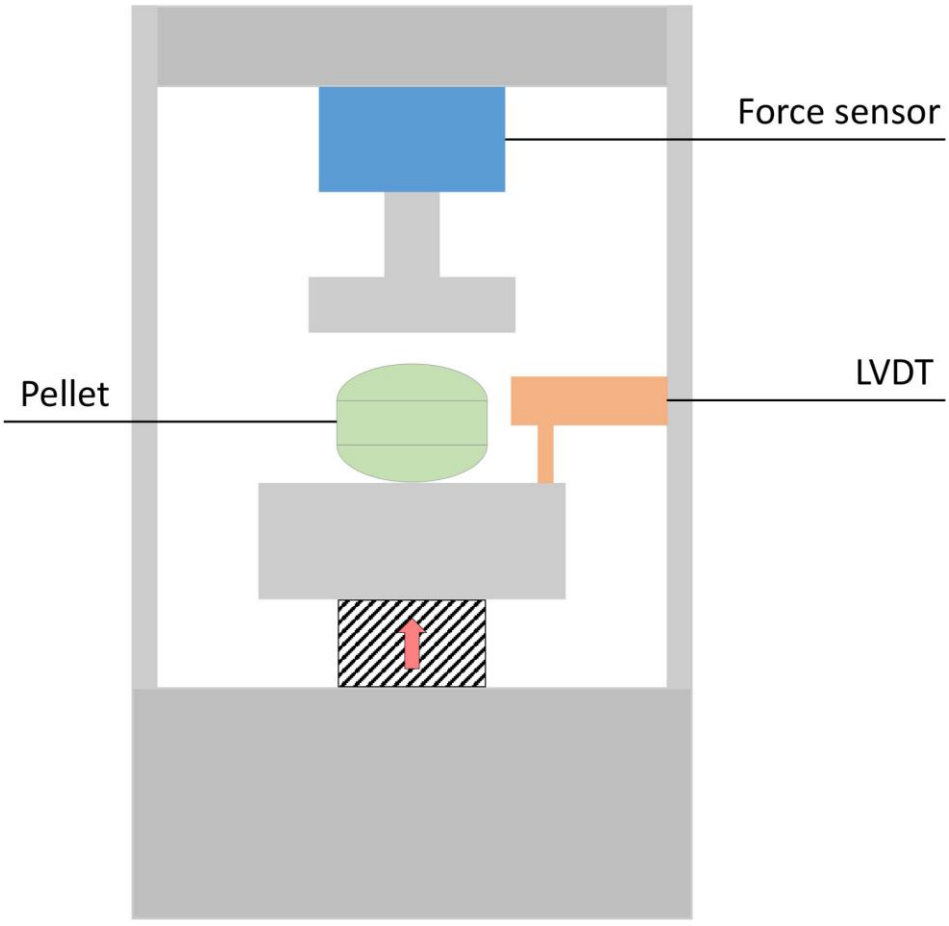

Figure_2_b.tif

Accepted manuscript doi:
10.1680/jgele.18.00114

Accepted manuscript doi:
10.1680/jgele.18.00114

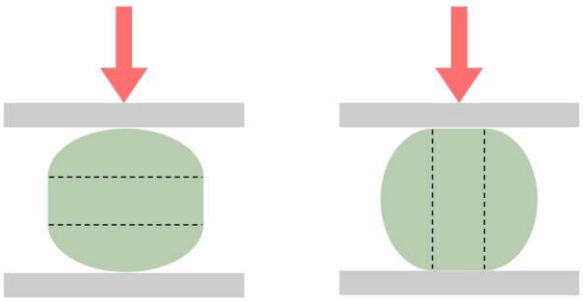

a) b)

Figure_3.tif

Accepted manuscript doi:
10.1680/jgele.18.00114

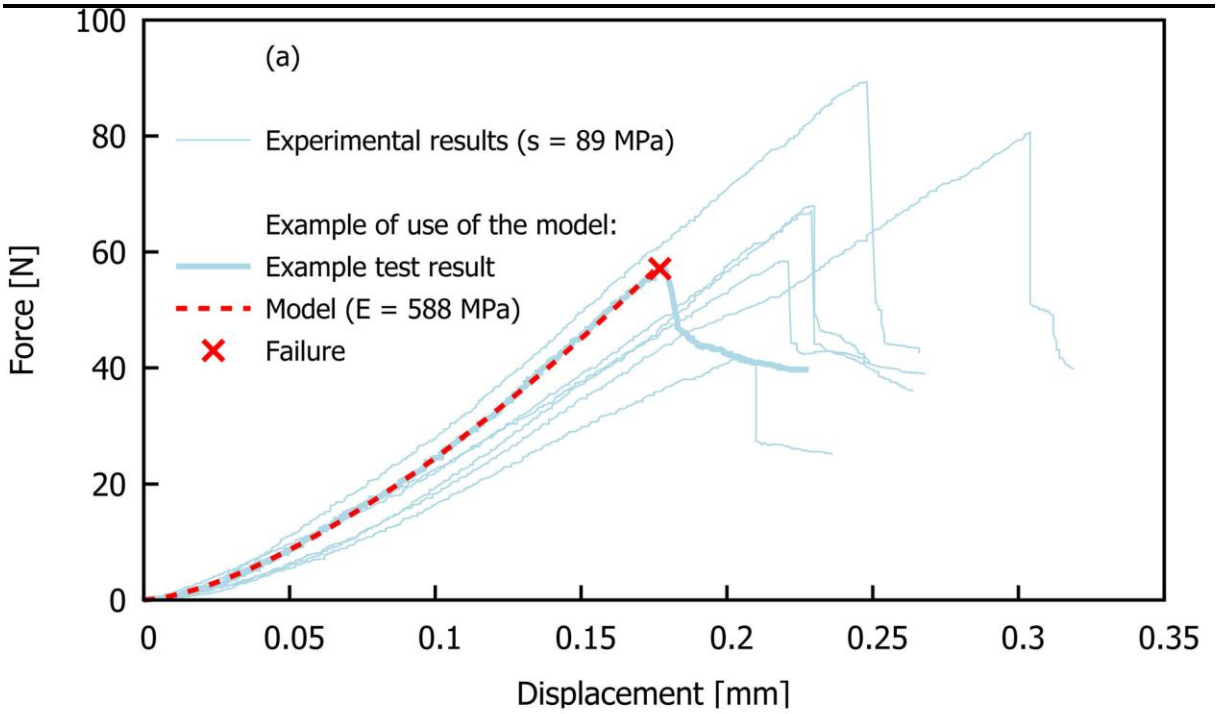

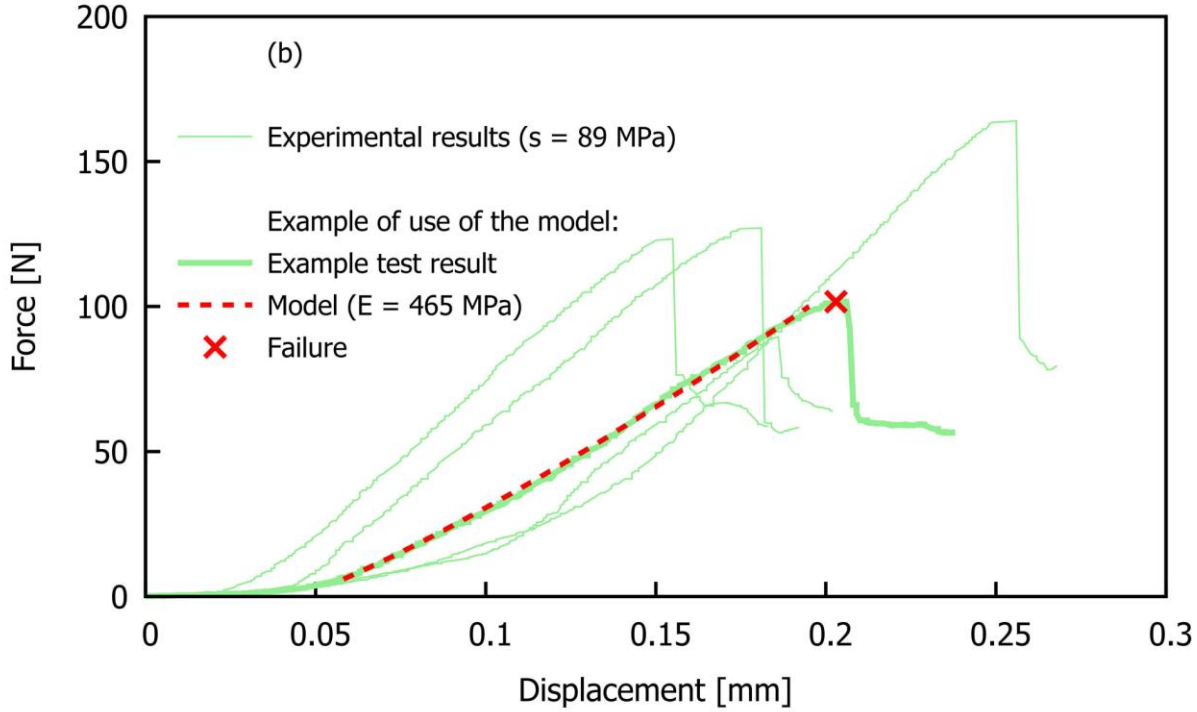

Figure_4_b.tif

Accepted manuscript doi:
10.1680/jgele.18.00114

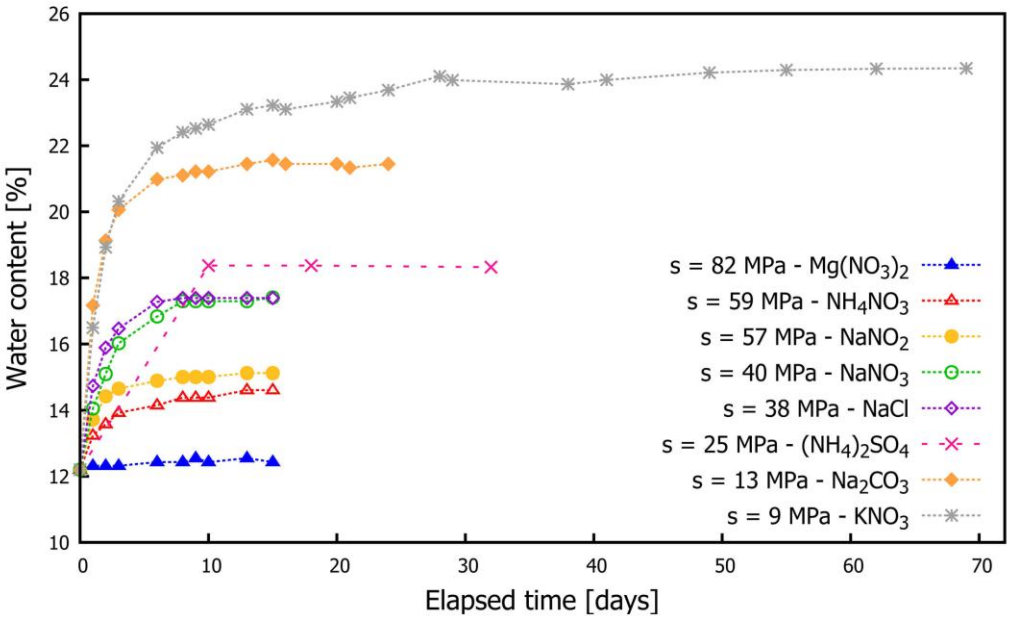

Figure_5.tif

Accepted manuscript doi:
10.1680/jgele.18.00114

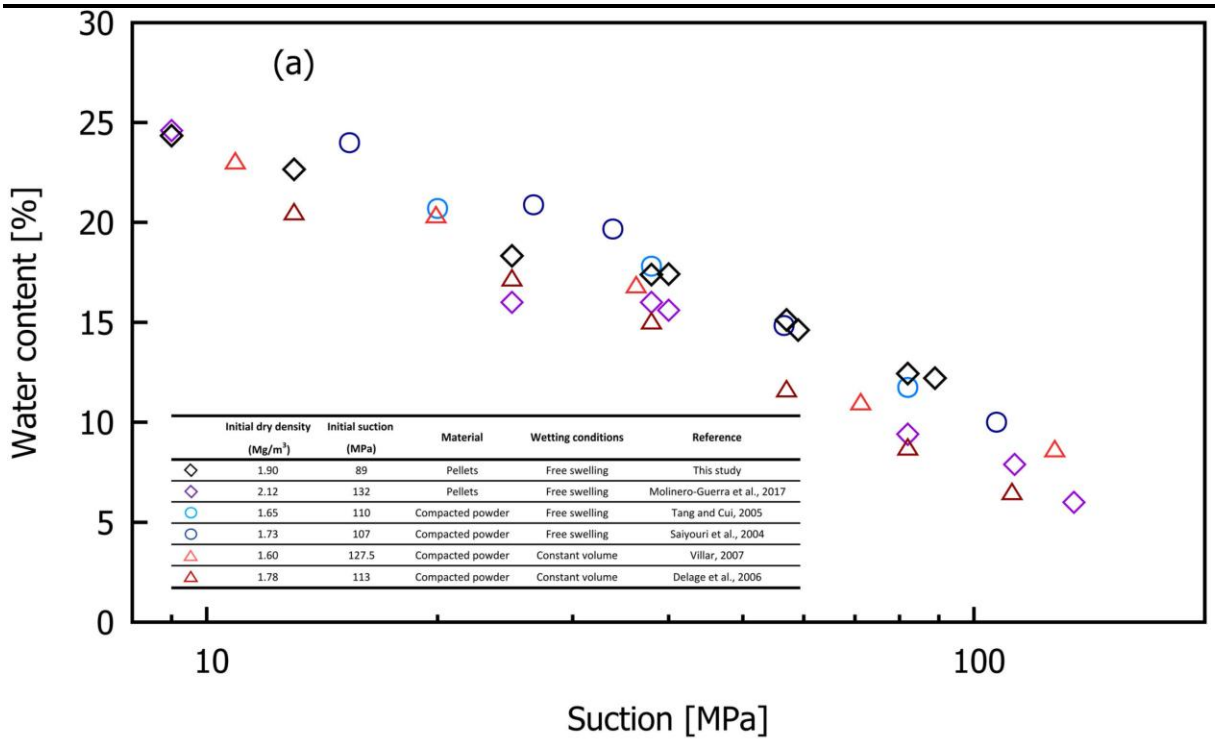

Initial dry density (Mg/m^3)	Initial suction (MPa)	Material	Wetting conditions	Reference
1.90	89	Pellets	Free swelling	This study
2.12	132	Pellets	Free swelling	Molinero-Guerra et al., 2017
1.65	110	Compacted powder	Free swelling	Tang and Cui, 2005
1.73	107	Compacted powder	Free swelling	Saiyouri et al., 2004
1.60	127.5	Compacted powder	Constant volume	Villar, 2007
1.78	113	Compacted powder	Constant volume	Delage et al., 2006

Figure_6_a.tif

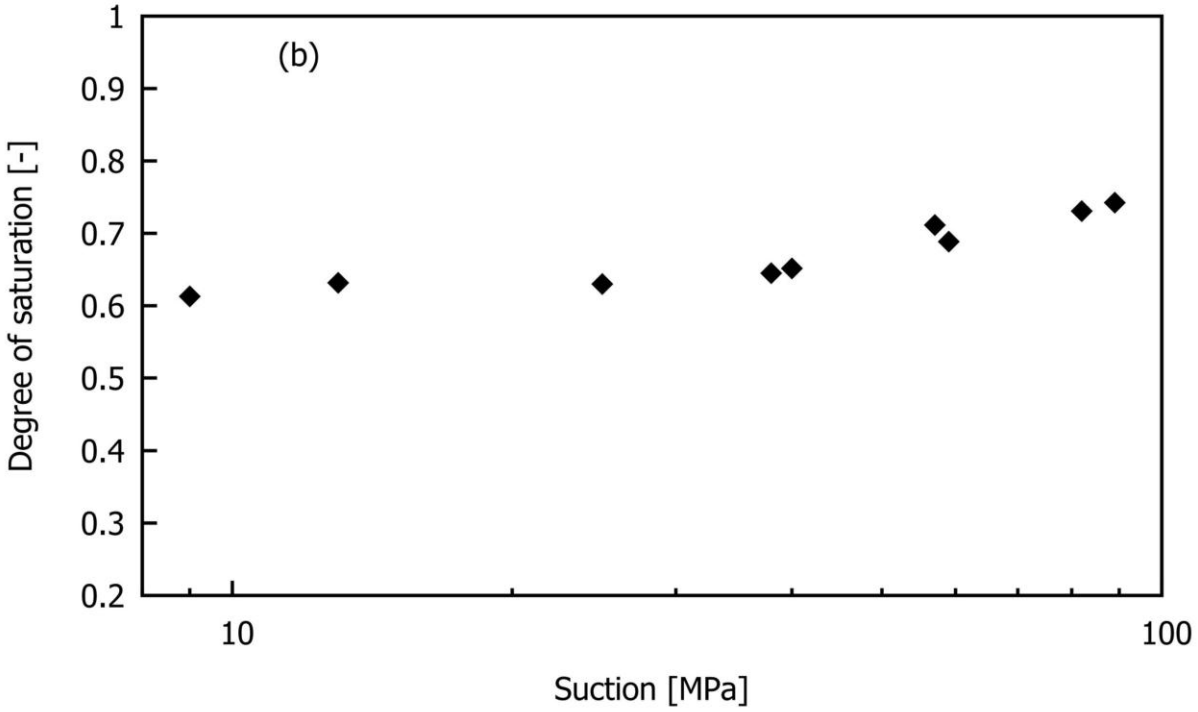

Figure_6_b.tif

Accepted manuscript doi:
10.1680/jgele.18.00114

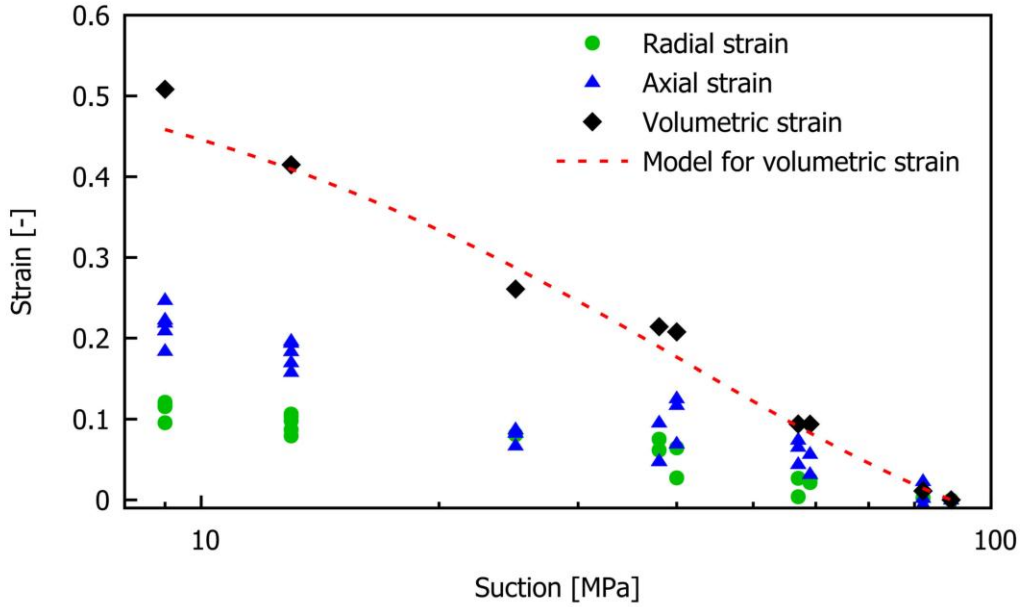

Figure_7.tif

Accepted manuscript doi:
10.1680/jgele.18.00114

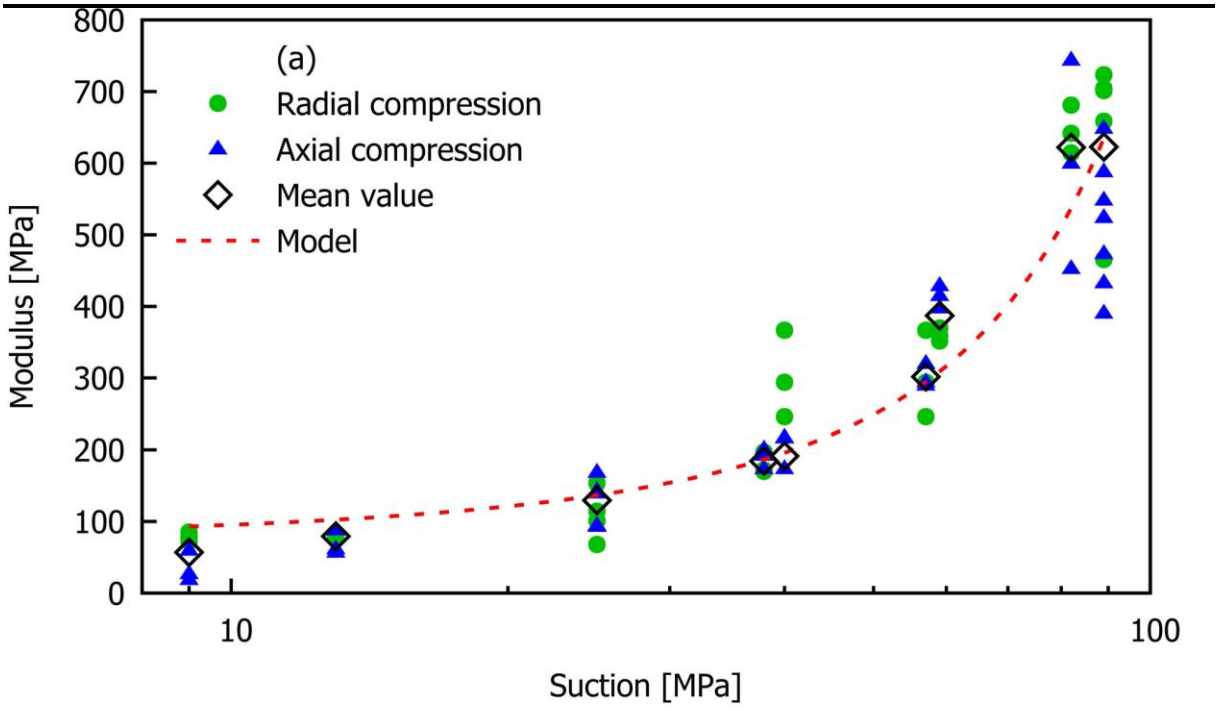

Figure_8_a.tif

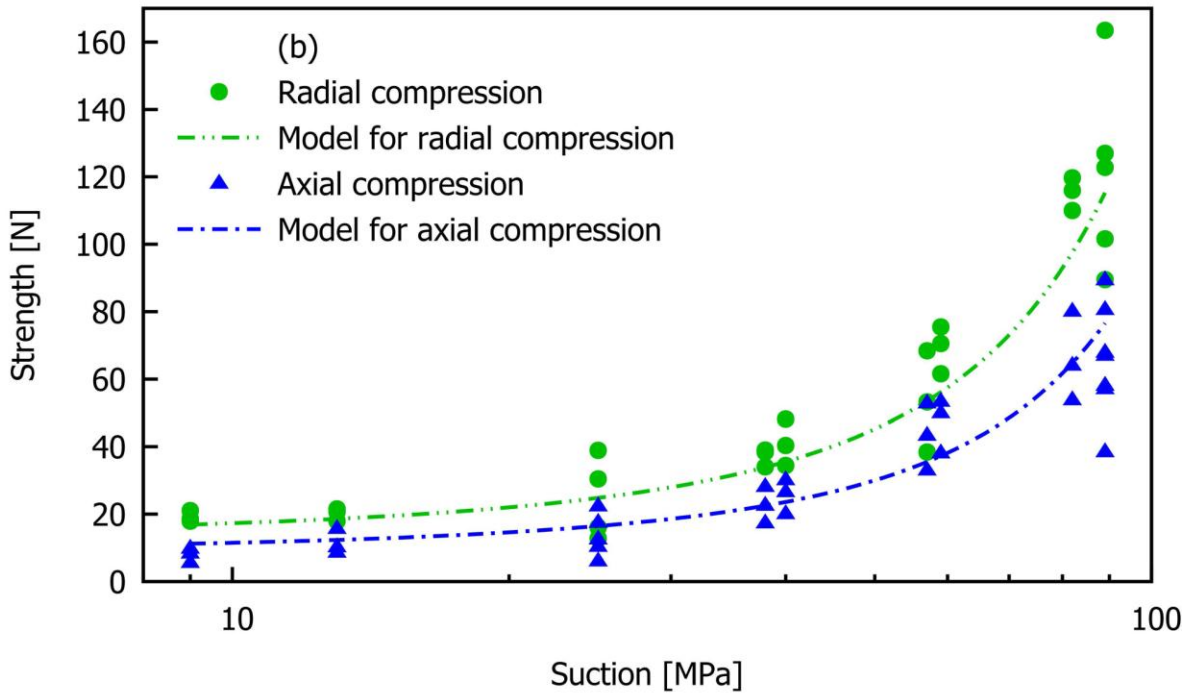

Figure_8_b.tif

Accepted manuscript doi:
10.1680/jgele.18.00114

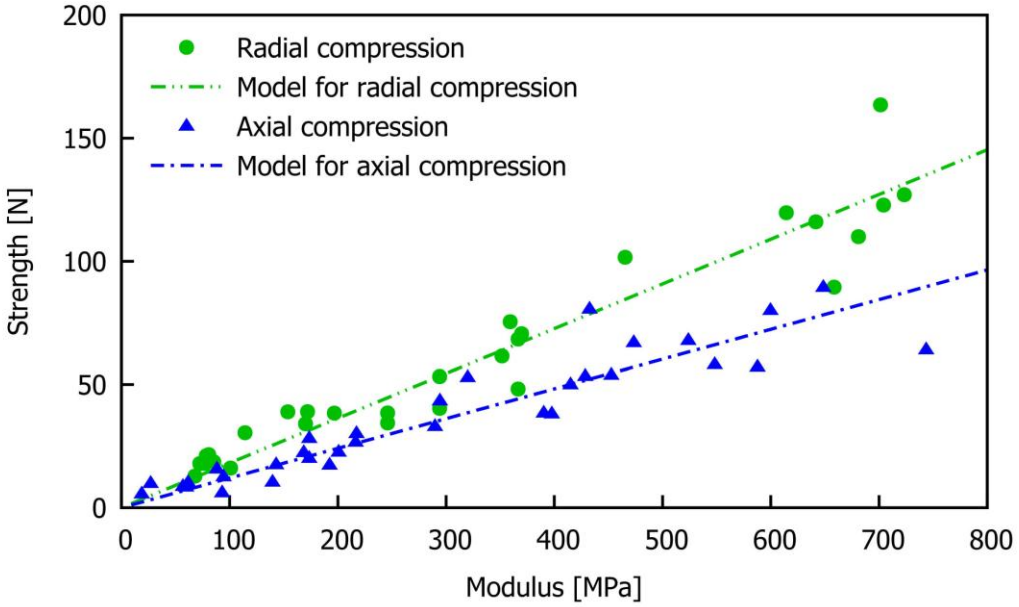

Figure_9.tif